JOURNAL OF
biomaterials
applications

Journal of Biomaterials Applications
0(0) 1–16

DOI: 10.1177/0885328217735049
journals.sagepub.com/home/jba
SAGE

Designing cellulosic and nanocellulosic sensors for interface with a protease sequestrant wound-dressing prototype: Implications of material selection for dressing and protease sensor design

Krystal R Fontenot[1], J Vincent Edwards[1], David Haldane[2], Nicole Pircher[3], Falk Liebner[3], Brian D Condon[1], Huzaifah Qureshi[4] and Dorne Yager[4]

Abstract

Interfacing nanocellulosic-based biosensors with chronic wound dressings for protease point of care diagnostics combines functional material properties of high specific surface area, appropriate surface charge, and hydrophilicity with biocompatibility to the wound environment. Combining a protease sensor with a dressing is consistent with the concept of an intelligent dressing, which has been a goal of wound-dressing design for more than a quarter century. We present here biosensors with a nanocellulosic transducer surface (nanocrystals, nanocellulose composites, and nanocellulosic aerogels) immobilized with a fluorescent elastase tripeptide or tetrapeptide biomolecule, which has selectivity and affinity for human neutrophil elastase present in chronic wound fluid. The specific surface area of the materials correlates with a greater loading of the elastase peptide substrate. Nitrogen adsorption and mercury intrusion studies revealed gas permeable systems with different porosities (28–98%) and pore sizes (2–50 nm, 210 μm) respectively, which influence water vapor transmission rates. A correlation between zeta potential values and the degree of protease sequestration imply that the greater the negative surface charge of the nanomaterials, the greater the sequestration of positively charged neutrophil proteases. The biosensors gave detection sensitivities of 0.015–0.13 units/ml, which are at detectable human neutrophil elastase levels present in chronic wound fluid. Thus, the physical and interactive biochemical properties of the nano-based biosensors are suitable for interfacing with protease sequestrant prototype wound dressings. A discussion of the relevance of protease sensors and cellulose nanomaterials to current chronic wound dressing design and technology is included.

Keywords

Chronic wounds, intelligent dressings, biosensor, nanocellulose, human neutrophil elastase, proteases, peptides

Introduction

Chronic wounds are a major clinical problem with an estimated 40 million people suffering from them worldwide, and one of the most costly health care problems today.[1] Chronic wounds are stalled in the inflammatory phase of wound healing, which extends beyond the 21-day cycle of acute wounds, and may be prolonged indefinitely.[2–4] Local and systemic factors can contribute to the development of different types of chronic wounds including venous, pressure, arterial, or diabetic ulcers.[2,5] On a molecular level, chronic wound fluid is

[1]Southern Regional Research Center, USDA, New Orleans, LA, USA
[2]Innovatech Engineering, Tallahassee, FL, USA
[3]University of Natural Resources and Life Sciences, Vienna, Austria
[4]Plastic and Reconstructive Surgery, Virginia Commonwealth University, Richmond, VA, USA

Corresponding author:
J Vincent Edwards, Southern Regional Research Center, USDA, 1100 Robert E. Lee Blvd., New Orleans, LA, USA.
Email: vince.edwards@ars.usda.gov

comprised of cytokines, chemokines, growth factors, electrolytes, and proteolytic enzymes,[6–8] which are imbalanced and delay the normal wound-healing cascade.

Proteolytic enzymes including, matrix metalloproteases (MMPs) and serine proteases like neutrophil serine protease (human neutrophil elastase, HNE), are responsible for degradation of growth factors[9] and the extracellular matrix (ECM) proteins essential for epithelium closure. In general, acute wounds have normal levels of MMPs and HNE,[10,11] which facilitates the clearance of cellular debris. However, chronic wounds have elevated levels of MMPs (0.1–0.2 U/ml) and HNE (0.02–0.1 U/ml) depending on the type, i.e., diabetic, venous, pressure, and arterial ulcers.[12] Thus, elevated concentrations of MMPs and HNE delay the healing process and are also considered biomarkers for chronic wound treatment evaluation.[13–15]

Biosensors incorporate two critical components (i) a biomolecule (such as a peptide) and (ii) a transducer surface (carbohydrate, polyurethane, or polysaccharide). Conjugation of the substrate molecules with the transducer surface forms the apex of activation, which is triggered by a biochemical event giving rise to a detection signal.[16–18] Biosensors lie at the heart of point of care (POC) diagnostics. POC diagnostics, is becoming an increasingly significant tool in advanced chronic wound care, and POC protease evaluation has received considerable attention. In addition wound temperature, pH, bioburden, and moisture levels of the wound[19–21] are measurable indicators of pathology and hence the subject of dressing as well as sensor design.

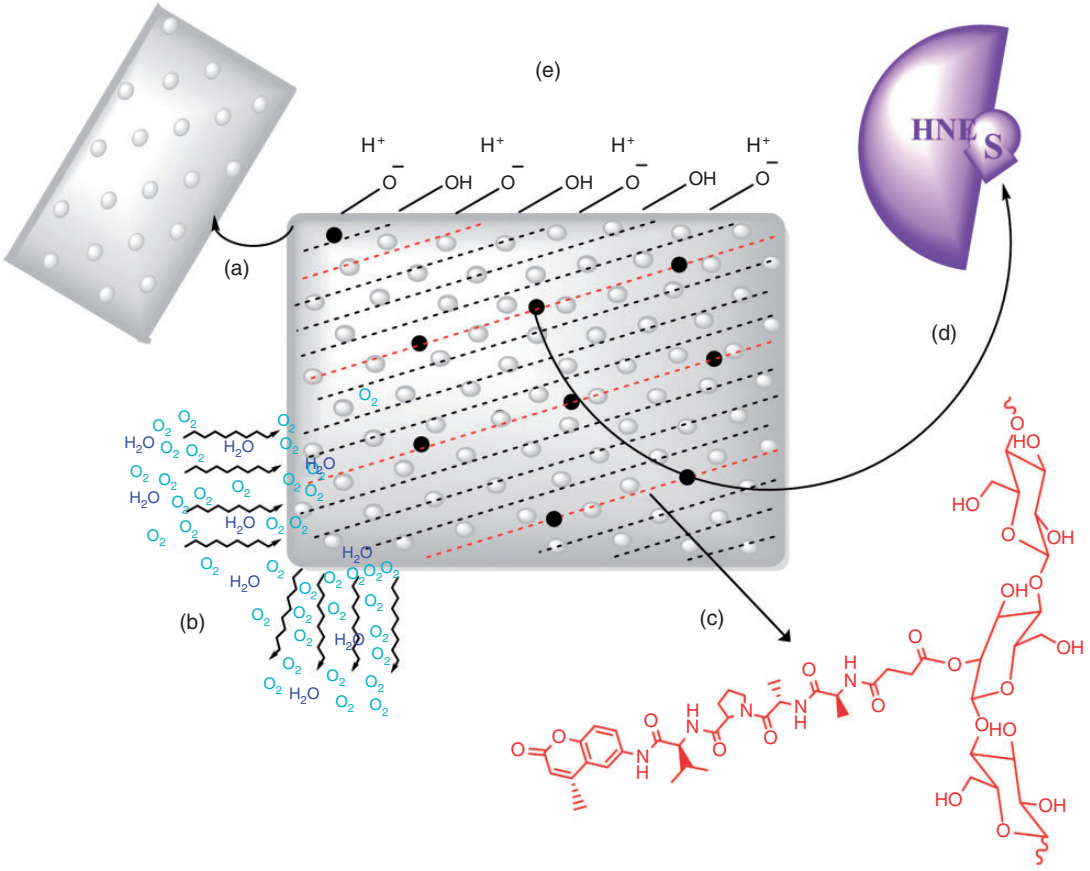

Figure 1. Depiction of select structural properties of a hypothetical intelligent semiocclusive chronic wound dressing. (a) The nanocellulosic materials possess a porous structure (porosity and pore size) and absorbency properties that facilitate exudate of the wound environment by maintaining a moist wound environment. (b) The porous structure enables the permeation of water and oxygen that enhance hydration and maintain moisture at the wound bed. (c) The fluorescent peptide substrate (Figure 2) is present throughout the wound dressing and is capable of detecting HNE at the threshold of the selected nanocellulose biosensor. (d) The release and detection of the fluorescent signal indicates the selective binding of HNE proteases with similar tailored fit of an enzyme–substrate complex (ES) enzyme bound to the peptide substrate and signifies the presence and biochemical imbalance of HNE in the chronic wound. (e) The anionic nanocellulosic biosensor surface acts as a sequestrant of the cationic HNE protease from the wound fluid as a way to remove the biochemical imbalance of excess HNE protease.

''Intelligent'' dressings may be defined as materials that respond to specific changes in the wound environment i.e. exudate volume, by altering structure or properties to bring about a useful result i.e. moist wound-healing conditions. The term was introduced a quarter century ago in the context of a material with self-adjusting water vapor rate of transmission properties.[22] Figure 1 diagrams moist wound healing, protease sequestration, and protease biomarker detection as well as other important concepts relevant to an intelligent dressing design that would ideally respond to a variety of biochemical or cellular cues in a chronic wound to facilitate development of a healing trajectory in the wound environment.

In this paper, POC diagnostic biosensors are combined with protease modulating dressings and applied to the detection of a protease biomarker. Given the concern over the role of unchecked proteolytic activity in chronic wounds, protease biomarkers are one set of indicators with an identified mechanism of action that underlies the pathology of nonhealing chronic wounds. Protease biomarkers have also received increased interest in a variety of inflammatory diseases.[23] The beneficial use of diagnostic or theranostic POC systems as is found with protease biomarkers is the ability to predict early outcomes, gauge the healing prognosis of the wound, and improve assessment of the effectiveness of wound care treatment[24] i.e. the healing or nonhealing trajectory of the wound.[12] A diagnostic POC sensor is designed to detect a specific biomarker, whereas a theranostic POC approach assists in guiding treatment.[11,25,26] Thus, protease sensors may be considered applicable as diagnostic or theranostic depending on the clinical treatment goals. Here the focus is on elevated HNE as a chronic wound protease biomarker.

It is important to note that a number of creative approaches to dressing/sensor motifs have been reported in the literature, which addresses some of the issues of an in situ protease sensor/sequestrant dressing identified in this paper. Reports based on gauze dressing, hydrocolloids, and hydrogels have recently shown the potential for applying an enzyme sensor/dressing paradigm. They all involve detecting chronic wound protein biomarkers using an in situ POC diagnostic approach. Derikvand et al. prepared an esterase substrate biosensor by immobilizing a fluorogenic moiety directly onto cellulosic gauze using click chemistry (copper (I)-catalyzed azide–alkyne cycloaddition, CuAAC). Immobilization of the fluorophore to the cellulose substrate is designed to prevent the release of the fluorophore into the wound, and a biomolecule that is putatively biodegradable is released instead.[27] This type of approach also has potential as a signal-release design that could be used to monitor release of a therapeutic molecule into the wound. Patrick and Ulijn[28] assembled a hydrogel capable of detecting and removing proteases from solution. A poly(ethylene glycol acrylamide) cross-linked polymer (PEGA) hydrogel was conjugated to a peptide sequence flanked with a fluorescence resonant energy transfer (FRET) with a donor/acceptor pair. The peptide sequence specific for detecting HNE or MMP,[29] developed an evanescent wave fiber optic sensor to quantify protease activity directly in the wound bed. Detection is based on degradation of thin gelatin films, which in the preparation are deposited on the fiber core that also serves as the protease substrate. Therefore, utilizing transducer surfaces immobilized with peptide substrates with an affinity for proteases is becoming an adaptable approach for potential wound dressing in situ POC diagnostics.

The biocompatible properties of cellulose are attributable in part to cellulose's low propensity to absorb proteins making it compliant in biological milieus.[30,31] In addition, we and others have shown that albumin, which is the protein of highest concentration in wounds, does not unfold on cellulosic materials.[32,33] The hydrophilic material and surface charge derives from an abundance of hydroxyl functionality present in the nanocellulose structure. As discussed above, the ability to combine measurable protease detection with a dressing motif that neutralizes the effect of proteases is one of the specific goals of wound-healing biomaterial design.[34] Therefore, we immobilized the fluorescent elastase tetrapeptide or tripeptide biomolecule substrate (Suc–Ala–Ala–Pro–Val–4-amido-7-methylcourmarin (AMC) or Suc–Ala–Pro–Ala–AMC) with specificity for the HNE-sensing element onto cellulosic cotton print cloth (CPC) and three nanocellulosic materials including cellulose nanocrystals (NCs), nanocellulose composites (NCCs), and nanocellulosic aerogels (NAs). These molecular sensor features are examined in the context of dressing/sensor properties like (i) porosity and pore size, water vapor transmission rate, (ii) specific surface area (SSA) as a function of loading the peptide substrate and protease sensitivity, and (iii) sequestration of HNE as it relates to surface charge of the material.

Materials and methods

Cellulosic and nanocellulosic transducer materials

Cellulose print cloth (CPC) is a lightweight mercerized bleached cotton fabric employed as a representative of a cellulosic transducer surface. The wood cellulose NCs were prepared using sulfuric acid hydrolysis of 100% wood pulp cellulose and purified using ultrafiltration, reverse osmosis, and cartridge style filters producing NCs with an average diameter of 5–10 nm and length of 50–60 nm.[35–39] The wood NCCs are comprised of

NC and microfibrillated cellulose (MFC) in a ratio of 50/50.[35–37] A description of the preparation of NCC was previously reported.[40] The NA was prepared by dissolving highly cleaned greige cotton in calcium thiocyanate octahydrate followed by casting/coagulation, regeneration, and supercritical carbon dioxide ($scCO_2$) drying.[41–44]

Esterification of transducers and immobilization of the fluorescent peptide substrate on the transducers

Edwards et al. previously outlined the esterification and peptide immobilization of the transducers.[40,45] The print cloth fabric (CPC) was pretreated as previously reported by Edwards et al.[40] Briefly, the CPC and nanocellulosic transducers: wood NCs, wood NCCs 50/50, and NA were esterified with Fmoc–Gly–OH with the respective coupling agents (Ethyl cyanoglyoxylate-2-oxime (Oxyma Pure), diisopropylcarbodiimide (DIC), and 4-dimethylaminopyridine (DMAP) in N, N-dimethylformamide (DMF) and sonicated. The materials were washed thrice by centrifuging or filtration with DMF or dichloromethane (DCM), and in select cases, allowed to air dry. (*Note:* the NA–Gly–Fmoc was allowed to remain in DMF for storage and was not air-dried.) The transducers CPC–Gly–Fmoc, NC–Gly–Fmoc, NCC–Gly–Fmoc, and NA–Gly–Fmoc were prepared for peptide coupling by deprotection or stored at ~4–8°C. A deblock solution (piperidine/DMF) was used to deprotect the Fmoc protecting group from the glycine-esterified transducers. (*Note:* the NA–Gly–Fmoc was washed with DMF prior to soaking in the deblock solution.) The materials were washed thrice by centrifuging or filtration with DMF, DCM, and in select cases allowed to air dry. (*Note:* the NA–Gly was washed thrice with DMF and then prepared for peptide coupling or stored in DMF for further use).

Peptide immobilization of CPC–Gly, NC–Gly, NCC–Gly, and NA–Gly was achieved by activating the tetrapeptide (Suc–Ala–Ala–Pro–Val–AMC) or tripeptide (Suc–Ala–Pro–Ala–AMC) substrates with DMAP in DMF for 20 min, to which Oxyma Pure and DIC were added. The solutions were bath sonicated for 3 h, placed in the refrigerator overnight, and purified by centrifuging or filtering thrice with DMF, DCM, or methanol (MeOH), and in select cases allowed to air dry. (*Note:* the peptide–nanocellulose aerogel (pNA) was washed thrice with DMF, thrice with phosphate buffer saline (PBS, and stored in PBS.) The biosensors were stored at ~4–8°C until further use. *Note:* ''biosensor'' denotes the glycine esterified transducer immobilized with the tetrapeptide or tripeptide substrate.

Removal of a small amount of peptide (Gly–(Succinyl)–Ala–Pro–Ala–AMC) from the peptide–cellulose conjugates was necessary to obtain mass spectroscopic characterization of the peptide–cellulose conjugate and demonstrate formation of the conjugate bond. Thus, upon the completion of drying, the cleavage of the peptide substrate from each cellulose and nanocellulose substrate material required the addition of a cleavage cocktail (trifluoroacetic acid (TFA)/water/triisopropylsilane), which reacted for 3 h. The cocktail solution from each biosensor was diluted (water/acetonitrile) and submitted for electrospray ionization liquid chromatography mass spectrometry (ESI-LC/MS) to confirm the intact sequence of the peptide component of the biosensor via its molecular weight i.e. mass spec parent ion: $[M + H] = 572.34$ for the tripeptide-linked portion Gly–(Succinyl)–Ala–Pro–Ala–AMC) of the conjugate.

Characterization of biosensors and material physical properties

Optical images of transducer. A Hirox optical microscope equipped with an MGX lens was used to obtain high range images with at a 350× magnification, a resolution of 0.5 μm, and a scale of 1000 μm of CPC and NC. A digital camera, Sony Cyber-shot full HD 1080, with a 10× optical zoom and 8.1 megapixels was used to image the NCC and the NA with a white background.

Elemental analysis. Elemental analysis of the matrices was calculated as previously reported.[40] All samples were submitted as solids to Midwest Microlabs for carbon (C), hydrogen (H), and nitrogen (N) analysis. The percentage of nitrogen content was used to calculate the peptide loading in μg/mg using Microsoft Excel 2007.

Degree of substitution (D.S.). The degree of substitution of the transducers was calculated using the Touzinsky and Gordon method[46] as previously reported.[40]

SSA. The SSA of the transducers were calculated as previously reported.[36,40,47,48] The SSA of the cellulose CPC was calculated using the volume of a cylinder divided by the weight of the matrix. The SSA of the NC was calculated based on the volume of cylinder, density formula, number of particles, the surface area of a cylinder, and the SSA formula. The SSA of the NCC and NA was determined using the Brunauer–Emmett–Teller method[47] with N_2 and Kr, respectively.

Porosity. The porosity of CPC and NCC was previously described.[49] The porosity of the NA was calculated using equation (1) where the density of the transducer

is divided by the density of cellulose skeletal density ($\rho_{SK} = 1.46\,g/cm^3$, $\rho = m/V$)

$$\text{Porosity} = \frac{1-\rho}{\rho SK} \times 100 \quad (1)$$

Moisture absorption and moisture vapor transmission rate (MVTR). The moisture absorption of the transducers was measured at 15, 30, 60, 90, 120, and 180 min after soaking in Millipore water. Each transducer was weighed, soaked in Millipore water, and removed after different time intervals, slightly dried with a Kimwipe, and weighed. After each time interval, the transducers were removed from the millipore water, slightly dried with a Kimwipe, and weighed. The swelling capacity of the transducers was determined using equation (2) where *Ws* is the weight of NA with absorbed water and *Wd* is the weight of dry NA. Precession Testing Inc. performed the water vapor transmission rate according to procedure B—water method at 23°C of the ASTM E96–95 method.

$$\text{Swelling}\,(\%) = \frac{(Ws - Wd)}{(Wd)} \times 100 \quad (2)$$

Surface charge. The zeta potential (ζ) of the peptide free transducers were assessed using a Malvern Zetasizer nano ZS90 (Malvern Inc., Massachusetts). The CPC, NCC, and NA were ground into powder using a Wig L Bug Ball Mill and pulsated for ~1.5 min. Stock solutions (5 mg/0.25 ml) of the ground transducers were prepared in Millipore water from which 1 mg/ml (CPC, NC, and NA) and 0.5 mg/ml (NCC) solutions were prepared. The respective solutions were sonicated for 2 h prior to obtaining triplicate zeta potential measurements.

Bioactivity characterization

Fluorogenic enzyme sensitivity assay. The sensitivity assay of the cellulosic and nanocellulosic materials employed was previously outlined by Fontenot et al.[49] Briefly, duplicates of ~2 mg of each biosensor were placed into a 96-well plate and 100 µl of PBS (0.5 M NaCl and 0.1 M NaH_2PO_4), pH 7.3 was added. A standard curve was constructed by employing peptide substrate solutions with a total volume of 150 µl at concentrations in the range of the peptide loading (see Table 1) and HNE ranging from 2 U/ml to 0.0156 U/ml. To start the reaction, 50 µl HNE ranging from 2 U/ml to 0.0156 U/ml was added to the 96-well microtiter plate containing the biosensors to provide a total volume of 150 µl. Fluorescent measurements at 37°C were monitored for 1 h at 1-min intervals using a Biotech Synergy HT with a tungsten halogen lamp and photomultiplier detection. The 96-well plate was shaken before each measurement for 3 s and the measurements were acquired at 360-nm excitation and 460-nm emission. The wound-like fluid comprised of PBS and HNE. The fluorescent measurements were processed in Microsoft Excel 2007 and the last measurement at 1 h was used to generate the bar graph with error bars.

Sequestration of elastase from wound-like fluid with transducers. The protocol from the sensitivity assay was modified for the sequestration assay. To 96-well plate, a standard curve (1–0.0156 µmol/ml) of the tetrapeptide or tripeptide substrate (200 µl) was added. To another set of wells, a 0.5 U/ml of HNE (100 µl) in PBS was added in duplicates to ~2 mg of the CPC, NC, NCC, NA, and Promogran (a commercially available sequestrant dressing) in a 96-well plate and allowed to sequester for 24 h at room temperature. After which, the transducers (CPC, NCC, NA, and the Promogran) were removed from each well and squeezed to remove excess solution. The volume of the HNE solution was

Table 1. Specific surface area, peptide loading, sensitivity, and surface charge values for the cellulose and nanocellulose materials.

Biosensors[a]	SSA[b] (m^2g^{-1})	Peptide[c] (µg/mg)	Sensitivity[d] (U/ml)	Surface charge[e] (mV)	% Protease sequestered
pCellulose print cloth	0.016	7.19	0.500	–11	17
pNanocrystals	261	88.13	0.015	–43	67
pNanocellulose composite	0.035	30.00	0.125	–12	17
pNanocellulose aerogel	156	20.31	0.125	–36	53

[a]The biosensor is defined as the nanocellulose material immobilized with a tetrapeptide (Suc–Ala–Ala–Pro–Val–AMC) or a tripeptide (Suc–Ala–Pro–Ala–AMC, aerogel).
[b]The specific surface area was determined by Brunner Emmett Teller nitrogen absorption.
[c]The peptide loading is based on percent nitrogen from element analysis and calculated based on formulas previously reported by Edwards et al.[30]
[d]The sensitivity values were obtained as reported in the Materials and methods section.
[e]The surface charge as determined by Zeta potential.

reverse pipetted and adjusted to 100 µl volume with PBS. The 100 µl of HNE with the NC was transferred to a micro-centrifuge tube, centrifuged, and the supernatant was transferred to a new well, reverse pipetted, and the volume was adjusted to 100 µl with PBS.

To start the reaction, 100 µl of HNE, 0.5 U/ml, was added to the wells containing the 200 µl volume of the tripeptide or tetrapeptide substrate standard curve for a total volume of 300 µl. Subsequently, 200 µl of 0.5 µmol/ml tripeptide or 0.125 µmol/ml of the tetrapeptide substrate solution was added to the biosensor wells to provide a total volume of 300 µl. Fluorescent measurements at 37°C were monitored for 1 h at 1-min intervals using a Biotech Synergy HT. The 96-well plate was shaken before each measurement for 3 s and the measurements were acquired at 360 nm excitation and 460 nm emission. The fluorescent measurements were processed in Microsoft Excel 2007 software program and the last measurement at 1 h was used to generate the bar graph with error bars.

Fibroblast cytotoxicity assay. To the nanocellulose and cellulose peptide conjugate materials (2 mg), a total of 1 ml of Dulbecco's Modified Eagle's Medium (DMEM) without bovine serum, was added. Initially, 0.5 ml of medium was added to the samples and allowed to sit for a few minutes after vortexing. An additional 0.5 ml of medium was then added, the mixtures were vortexed for 2 min, and were finally sonicated for 10 min. Then, the samples were incubated in the dark overnight. Samples were centrifuged at ~20,000 g at 4°C for 15 min. Serum was added to ~500 µL of the supernatant, to a final concentration of 10%. In triplicate, 100 µL of the serum containing supernatant was added to confluent fibroblasts in a 96-well microplate. The plates were incubated overnight in a CO_2 incubator. Promega MTS reagent was added to the treated fibroblasts. An initial optical density (O.D.) was measured at 495 nm, the plate was incubated for 30 min, and the O.D. was measured again at 495 nm. To calculate the formazan produced, the initial O.D. for each well was subtracted from its final O.D.

Results and discussion

Selection of transducer surfaces for protease sensor/dressing material

Each material evaluated as a protease sensor transducer surface has structural and biophysical characteristics that influence its functional properties, sensor sensitivity, and interface compatibility with a dressing. Figure 2 depicts the range of cellulosic (print cloth, CPC, as a control) and nanocellulosic materials presented in different physical forms such as NCs, NCCs, and NAs.

The type of transducer surface selected for dressing interface depends on the environment of the wound and compatibility with semiocclusive or moist healing dressings, i.e., thin films, hydrogels, alginates, hydrocolloids,

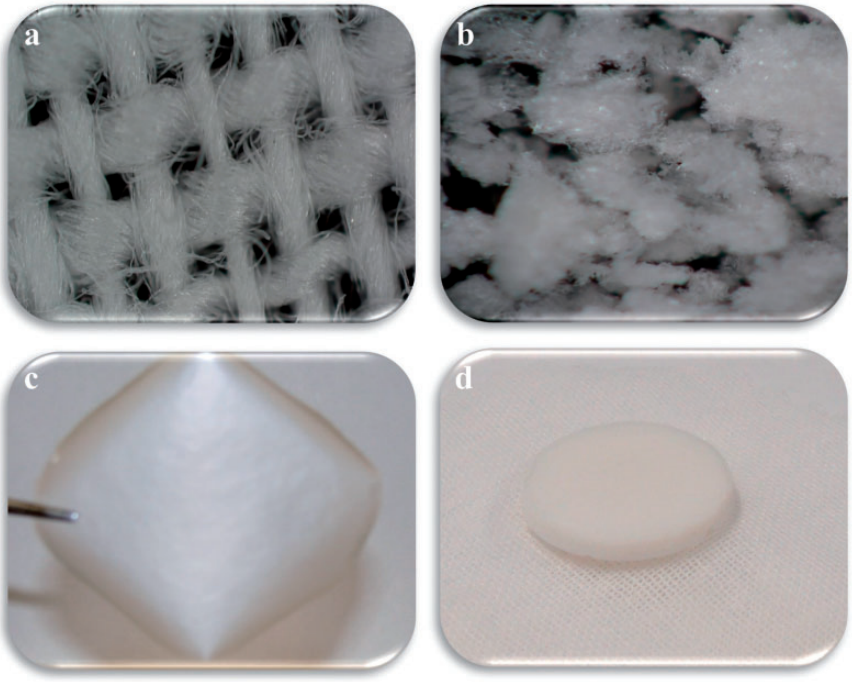

Figure 2. Optical images of (a) CPC, (b) NC, (c) NCC, and (d) NA.

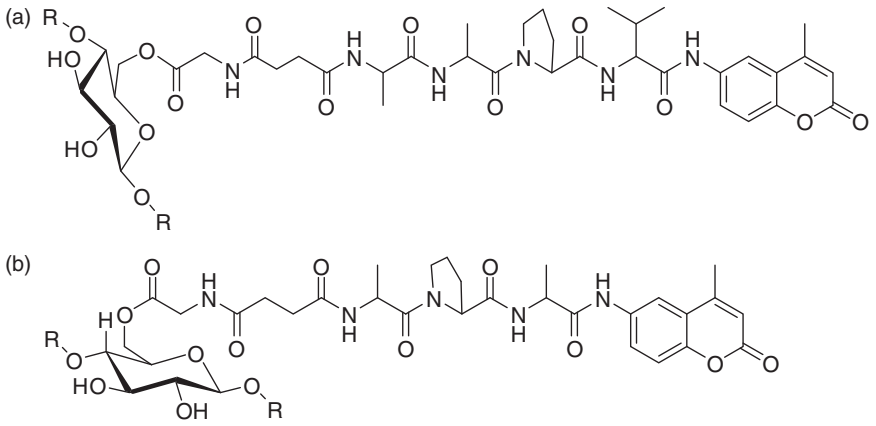

Figure 3. Structure of the (a) tetrapeptide (Suc–Ala–Ala–Pro–Val–AMC) and (b) tripeptide (Suc–Ala–Pro–Ala–AMC) substrate anchored on to glycine-esterified cellulosic or nanocellulosic materials.

or gauze. Thus, the property design that consists of texture, thickness, wettability, and porosity in the material composition of the sensor plays an important role in sensor selection as a compatible interface with the dressing. For example, the CPC fabric prepared from cotton fibers offers a planar surface with a woven cross pattern structure that would be compatible with a woven, nonwoven, or fibrous wound contact layer. With regard to the nanocellulosic materials, the nanocrystalline cellulose presents as a powder which as seen with SEM contains crystals that have a geometrical rod-like shape. A previous report has addressed an approach to interfacing nanocrystalline protease sensors in powder form with dressings through interface of a cellulose membrane, filtration layer that deposits the dialyzed protease from wound fluid on the sensor surface by way of size exclusion filtration.[50] The combination of cellulose NCs and MFC into a composite with a ratio of (50/50:NC/MFC) yields the NCC μporous, paper-like film, which was developed to provide a solid material nanocellulosic interface with dressings.[40] Similarly, the NA is a lightweight solid material with an open porous interconnected structure, which may be prepared from raw greige cotton[44] and is compatible with highly exudative wounds.

Synthesis and physical properties of the biosensor layer

The synthesis of some of the sensor components and preparation of the materials has been previously described.[40,44,49] The cellulosic and nanocellulosic transducers were covalently modified with a fluorescent peptide substrate using peptide coupling chemistry, as previously reported.[30,40,44,49] Figure 3 exhibits the structural profile of the fluorescent tripeptide (Suc–Ala–Pro–Ala–AMC) and tetrapeptide (Suc–Ala–Ala–Pro–Val–AMC) elastase substrates conjugated to the cellulosic or nanocellulosic materials. Immobilization of the peptide substrate via the cellulosic hydroxyl group was accomplished through glycine esterification of the COOH-terminal carboxyl group attached to cellulosic hydroxyls, leaving the N-terminus of the glycine amino functionality for peptide conjugation. The succinyl group (Suc) of the peptide substrate is then attached to the amino group of glycine to give peptide–cellulose conjugates, which constitute the biosensor design of each of the materials (pCPC, pNC, pNCC, and pNA).

SSA and peptide loading on sensor

The cellulosic and nanocellulosic materials were evaluated for SSA and peptide-loading capacity (Table 1). The structure and SSA of the materials influence the quantitative loading of the fluorescent peptide substrate on the biosensor surface by way of the number of available cellulose hydroxymethyl groups. On the other hand, it is important to note that the hydroxymethyl groups that are the principle functionality of ester bond attachment to the sensor molecule may account for <2% of the available hydroxyl functionality on the surface of cellulosic-based materials.[51] Table 1 provides the SSA and peptide-loading values for the cellulose and nanocellulose materials, which rank as follows pNC > pNA > pNCC > pCPC (highest SSA to lowest). Accordingly, increasing the SSA of the materials results in a similar order of loading of the peptide substrates onto the transducer surface during the preparation of the sensor, which is shown in Figure 4. The pNC has the greatest peptide loading on a transducer surface. In general, CPC has a 2–13,000-fold lower SSA compared to the nanocellulosic biosensors. It is noteworthy that the reduction in the SSA of the pNCC is due to aggregation of the nanocrystalline particles blended with the microcrystalline particles.[40] On the other hand, the pNA has a relatively high SSA, but it

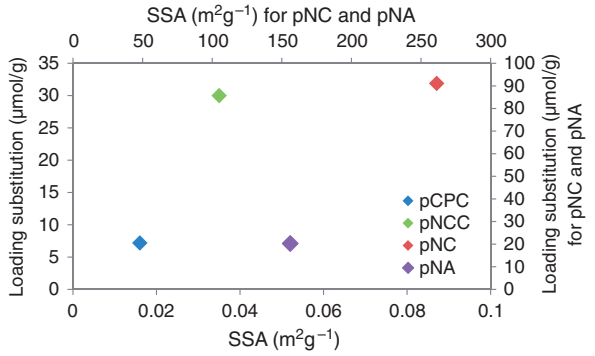

Figure 4. Graph of loading substitution plotted versed the SSA of the biosensors. The secondary axis shows the loading versus SSA for the pNC and pNA due to its higher SSA. An increase in the SSA results in an enhancement of peptide loading.

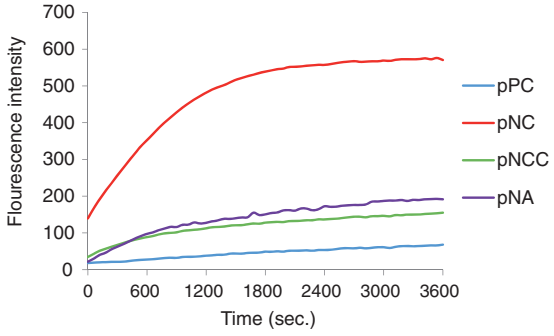

Figure 5. Reaction progress curves of human neutrophil elastase (HNE) with biosensors. Each reaction is the real-time fluorescent imaging based on the reaction of .5 units/ml HNE with 2 mg of biosensor.

has a lower peptide loading, which is attributed to the relatively small pore sizes (≥2–50 nm) within the NA structure. Thus, the nanocellulosic surfaces are primarily preferred as transducer surfaces for increasing peptide loading.

Sensor bioactivity, sensitivity, and elevated HNE levels in chronic wounds

The biosensors elastase activity is shown in Figure 5 as HNE reaction progress curves, which plots the enzyme's reaction with the cellulosic and nanocellulosic peptide conjugates by way of fluorescence as a function of fluorophore release. The HNE/peptide–cellulose conjugate reaction progress curves demonstrate the relative levels of fluorescent signal emitted from each sensor with time.

The detection sensitivity of the HNE biosensors is a function of transducer surface properties and peptide recognition sequence, which confer affinity for the

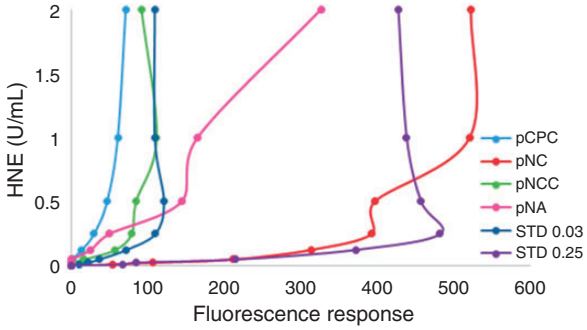

Figure 6. The fluorescence response of the cellulose and nanocellulose biosensors with HNE protease. (a) Reaction progress curves of human neutrophil elastase (HNE) with biosensors. Each reaction is the real-time fluorescent imaging based on the reaction of .5 Units/ml HNE with 2 mg of biosensor. (b) Sensitivity graph of the biosensors with 2 mg of biosensor. Standard curves (STD) were run at 0.03 and 0.25 moles of peptide substrate.

protease. Figure 6 shows the sensitivity values that reflect enzyme activity at the lowest concentration. The order of the detection sensitivities was found to be pNC > pNA > pNCC > pCPC. The general order of sensitivity correlates with transducer surface SSA as discussed above, and the levels of enzyme activity.

The cellulose nanocrystaline sensor (pNC) is the most sensitive protease biosensor of those examined here,[50] which is consistent with a higher SSA and also parallels the peptide loading on the material (Figure 4). The nanocellulosic sensors also appear promising for use in chronic wound protease detection considering that the HNE detection sensitivities of the nanocellulose biosensors range from 0.015 U/ml to 0.5 U/ml. Thus, the nanocellulosic sensors are within the range to detect HNE levels comparable to those found in chronic wound fluid, see Table 1.

Relationship of sensor sensitivity to protease activity in chronic wound fluid

Recent reports on protease diagnostic studies describe sensitivity and specificity in the context of the ability to identify chronic and healing wounds, respectively.[12] When analyzed for best classification of sensitivity and specificity of a nonhealing trajectory, the minimum elevated HNE range that characterizes a chronic wound was reported as 0.35–0.78 mU/110 μl. This observation is also consistent with Yager et al. who showed that pressure ulcer wounds have elastase activity in the range of 1–50 mU/ml[10] and the earlier report by Trengove et al.[52] where 500 mg/ml HNE was noted. The level of HNE was also found to depend on the type of chronic wound (diabetic, venous pressure, and

arterial ulcers).[12] Accordingly, based on the HNE activities that the sensors of this study detect, and the transducer surfaces evaluated here, the detection sensitivity of pNC detects HNE activity at levels present in most types of chronic wounds as listed.[12] On the other hand, the elastase sensitivities of the pNCC and pNA seem to fall within the range indicated by the same report for elevated HNE levels in arterial ulcers: median HNE levels in arterial ulcers were (110 mU/ml).[12]

Surface charge of biosensors and its effect on protease sequestration

The cellulose and nanocellulose materials each demonstrated varying levels of protease sequestration activity. Figure 7(a) shows the percent of HNE protease sequestered from wound-like fluid with the cellulose transducer (CPC), nanocellulose transducers (NC, NCC, and NA), and they are contrasted with a protease-modulating dressing that is currently employed clinically. Each transducer surface was assessed for its ability to actively sequester HNE protease from wound-like fluid over a 24-h time period. The transducers sequestered 17–67% of cationic HNE protease from the mimicked wound fluid during a 24-h incubation period.[45,53] The materials possessed the following order of sequestration activity pNC > pNA > pNCC > pCPC. The proposed nanocellulosic materials, as well as the cellulose CPC, have a 1- to 5-fold increase in protease sequestration compared with the clinical protease sequestrant dressing that was assessed (Figure 7(a)). Furthermore, the percentage of sequestration correlates with the surface charge values of each material, which indicates that a higher negative surface charge, leads to an increase in protease sequestration as shown in Figure 7(b).

Previously it has been shown that protease sequestration dressings with a net negative charge under wound conditions remove positively charged serine proteases as HNE from chronic wound fluid.[54,55] Thus, negatively charged materials consistent with phosphorylation, sulfonation, and oxidation, form a salt bridge with the cationic serine proteases like HNE by way of positively charged side chains of the proteins amino acids, i.e., arginine.[54,56–58] Accordingly, the surface charge of each of the materials of this study was determined by evaluating the zeta potential to determine the relation of charge to elastase sequestration or binding to the material. Both the cellulose and nanocellulosic transducers have negatively charged surfaces as listed in Table 1. The nanocellulosic transducers have a greater surface charge ranging from −12 to −42 mV compared to CPC (−11 mV) as determined by the Zeta plateau for each material.

Water vapor transmission rates of dressings and Fibroblast compatibility of sensor materials

The importance of water vapor transmission rates in wound dressings has historical roots in the landmark paper of Winter[59] demonstrating that moist wounds heal faster than dry wounds. Thus, the principle goal of chronic wound dressing design has been to modulate moisture in the wound bed to create a more optimal environment for healing. Following Winter's Nature paper, ensuing generations of dressing design led to different types of materials that progressed to what is referred to as a semiocclusive motif, which promotes a moist wound bed with no maceration by modulating the moisture vapor transmission rate MVTR.

Semiocclusive dressings and their constituent materials are in seven separate categories based on selected treatment and materials suitable for the wide range of exudative chronic wounds that exist.[19,60] For example, a minimally exudative wound may require a hydrogel, which is composed of a hygroscopic polymeric material; a moderately exudative wound, a hydrocolloid, which is semipermeable and absorbent; and an excessively exudative wound, an alginate capable of high water uptake and ion exchange to preclude adherence.[60] Other favorable properties of dressings requisite for maintaining a moist environment at the wound bed include modulation of gas exchange (oxygen and moisture), acting as a barrier for microorganisms, removing wound fluid, and nonadherence to the wound bed upon removal of the dressing.[61,62] Accordingly, the materials of this study are grouped by way of compatibility with semiocclusive dressings. Semiocclusive dressings utilize structural properties like porosity, permeability, polarity, and absorbency to maintain moisture and allow gas exchange such as oxygen and water vapor.[61,62]

The correlation of water vapor transmission rate (WVTR) and porosity also aligns with the dressing's water uptake. Recently, Xu et al. have reported a polyurethane-based dressing with moderate porosity that demonstrates biochemical and cellular markers for a peak-accelerated healing rate at an optimal WVTR of 2038 $g/m^{-2}\,d^{-1}$ in full thickness wounds.[63] In Figure 8, percent water uptake by the putative sensor/dressing material is compared with the percent water uptake rates of a clinical semiocclusive dressing that also functions as a protease modulating dressing. The range of water uptake of the nanocellulosic materials was from 250% to 1000%. Properties of porosity, pore size, water vapor transmission rate, and wettability directly affect the semiocclusive value of moist wound healing. Therefore, from a perspective of accelerating or enhancing a more favorable environment for healing, the properties as outlined and listed in Table 2 reflect the potential function of materials of this study in

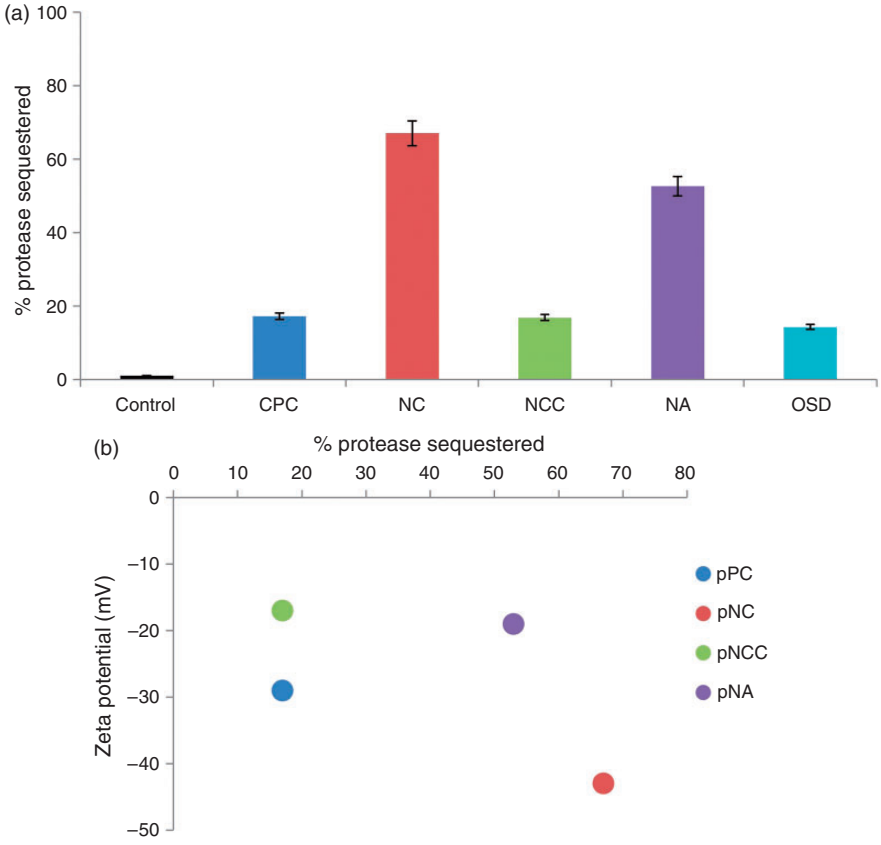

Figure 7. Graph of cellulose and nanocellulose materials as protease sequestrant materials. (a) Percent of HNE protease sequestered from wound-like fluid with cellulose-based transducers including CPC, NC, NCC, NA, and the commercially available oxidized sequestrant dressing. (b) Graph of zeta potential plotted versus the percent of protease sequestered from the transducers.

Table 2. Porosity and pore size values of the transducer surfaces.

Transducer surfaces[a]	Porosity[b] (%)	Pore size[c] (nm)	WVTR at 24 h[d] ($gm^{-2}d^{-2}$)	Wettability[e] (Contact angle°)
Cellulose print cloth	58	210 μm	674	<5
Nanocellulose composite	28	33	553	79
Nanocellulose aerogel	98	≥2–50	–	<5

[a]The transducer surface is defined as the nanocellulose material without any alteration or attachment of peptide substrate.
[b]The porosity of the cellulose print cloth fabric and the nanocellulosic aerogel were calculated using equation (1) and porosity of the nanocellulose composite was determined using mercury intrusion.
[c]The pore size measurements of the cellulose print cloth were obtained using a Hirox microscope by measuring the diameter of several cross-stitchings, the average pore size of the nanocellulose composite as determined using mercury intrusion, and pore size of the nanocellulosic aerogels as determined by gas adsorption.
[d]The water vapor transmission rate according to the ASTM E96-95 method B.
[e]The wettability of the materials was determined using contact angle measurements.

minimally exudative wounds due to the range of water vapor transmission rates, which is in the range of 522–674 $g\,m^{-2}d^{-1}$.

Moreover, the moisture absorption of the materials rank in the following order NA>, CPC>, and NCC, and the MVTR and porosity values are consistent with this. As shown in Table 2, the NCC has a MVTR of ~553 $g\,m^{-2}d^{-1}$ that is commensurate with levels associated with gas exchange at the wound bed for other types of commercially available thin films with an MVTR ranging from 400 to 800 $g\,m^{-2}d^{-1}$.[58,64] Similarly, the CPC has an MVTR within the same

range (674 g $m^{-2}d^{-1}$). On the other hand, the NCC has a twofold reduction in moisture absorption compared to the CPC. The NA, which has a greater porosity (98%) allows for a fourfold greater absorption of wound-like fluid compared to the NCC and a twofold increase compared to the CPC. Therefore, the three-dimensional structure of the NA provides the greatest capacity for moisture absorption uptake, which is also consistent with an increase in percent protease sequestration.

Water vapor transmission rates are a function of pore size, porosity, and material polarity (wettability). Tables 1 and 2 list the porosity, pore size, and relative polarity (Zeta Plateau) values of the cellulose and nanocellulose transducers. The larger pore sizes (210 µm) and a moderate porosity (58%) of CPC enable increased wicking of wound-like fluid into its structure. The nanocellulose materials have smaller pore sizes compared to cellulosic print cloth, however, increased porosity improves the swelling and water uptake. For instance, the NCC has a 25% porosity and a 33-nm pore size, which also influences the barrier and mechanical properties[65] of the system by allowing gas and moisture permeation[64,66,67] while abrogating entry of microbes. Hence, the materials of this study are viewed as having varying compatibility profiles with different types of semiocclusive dressings. The porous nature of both the NCC and NA and their relative wettability create a compatible design with semipermeable absorbent dressings like hydrocolloids and films. On the other hand, the increased swelling capacity of the aerogel (NA) would be compatible with an alginate or gauze dressing.

Experiments were also conducted to measure the effect of the sensor materials on dermal fibroblasts incubated overnight. As shown in Figure 8b formazan production was measured to assess cytotoxicity of the sensor materials to fibroblasts. No significant cytotoxicity of the materials on fibroblast growth and integrity was observed. Thus, preliminary assessments demonstrate the compatibility of the sensor materials with proliferative cells associated with initiation of wound healing.

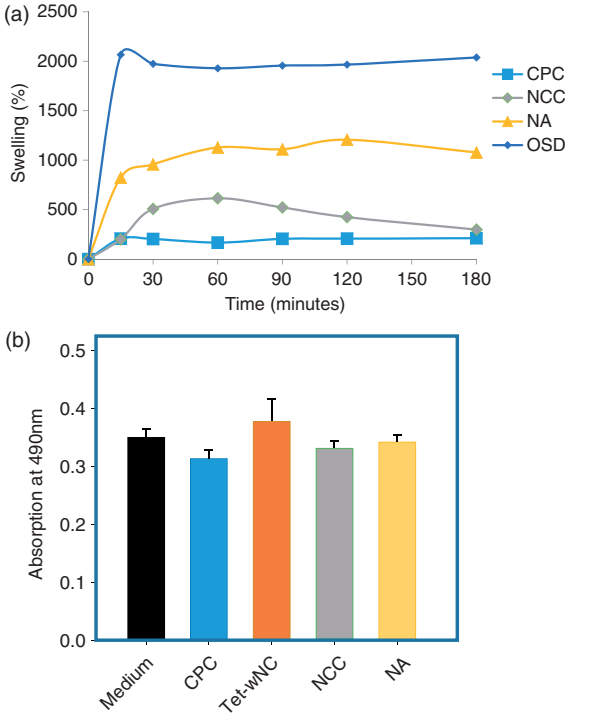

Figure 8. (a) Moisture absorption studies of CPC (blue), NCC (green), NA (yellow), and a commercially available oxidized sequestrant dressing (OSD, a composite of oxidized regenerated cellulose and collagen, navy). (b) Fibroblast cytotoxicity evaluation as outlined in the Materials and Methods section. The graph displays the Δ O.D.490 nm measured after Promega MTS reagent was added to sensor-treated fibroblasts, and incubated for 30 min to assess formazan production. Error bars represent SD. Tet-PC: tetrapeptide–cellulose analog on print cloth, Tet-wNC: tetrapeptide–nanocrsyalltine cellulose, Tet-NNC 50/50: tetrapeptide–nanocomposite 50/50, tripeptide–nanocellulosic aerogel.

Nanomaterial considerations in the design of a protease sensor/sequestrant dressing

The nanomaterials NCC and NA considered here are designed to improve the sensor properties afforded by nanocrystalline cellulose, and optimize these in a cellulosic nanomaterial design. For example, the free particle nature of the NCs maximizes the interaction with HNE and has the highest SSA and surface charge of the three materials, thereby yielding the highest sensitivity (0.015 U/ml) and protease sequestration (67%). The NCC offers presentation of nanocellulose as a film and was developed to provide an approach to transform the nanocellulosic crystals into a sheet-like material that will align with a material-layered interface at the wound contact layer (Figure 9). However, the difference in protease detection sensitivity between pNCC and pNC arises from particle aggregation of the NCs during the nanocomposite preparation process, which lowers SSA, and thus results in abrogation of protease binding to the pNCC transducer surface. Thus, the incorporation of the NCs into the pNCC provides a porous structure but a 7000-fold reduction in SSA (0.035 m^2g^{-1}) occurs.[40] The reduction in the SSA parallels the lower level of peptide loading and sensitivity (0.13 U/ml) as shown in Figure 3. However, the porous structure of NCC facilitates permeation of moisture vapor and gaseous molecules and may be adapted to contour with semiocclusive films, hydrocolloids, alginates, and gauze.

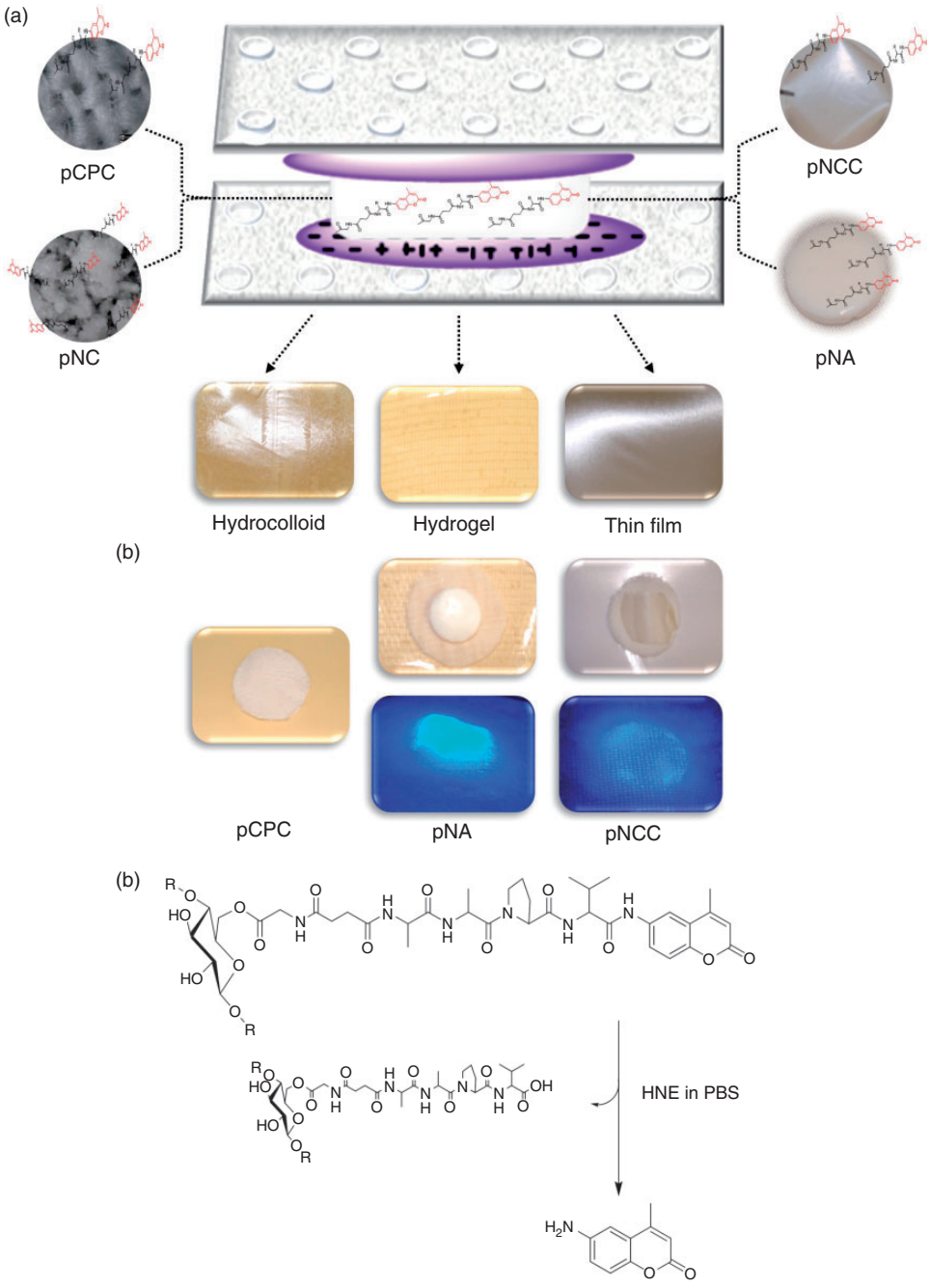

Figure 9. Illustration of (a) a multilayered semiocclusive protease dressing designed with fluorescent sensor, (b) depiction of the dressings without and with ultraviolet illumination, and (c) the mode of action pathway of the biosensor. Assembly of the sensors involves the following synthesis of peptide on cellulose or nanocellulose material -> characterization of peptide–cellulose conjugate (sensor) -> interface of sensor with dressing material. (a) The image of pCPC, pNCC, and pNA biosensors interfaced between two barrier layers and sandwiched between a contact and top layer of an intelligent protease dressing. The contact layer (hydrocolloid, hydrogel, or thin film) absorbs wound exudate and allows passage of wound fluid. The interchangeable nanocellulosic biosensor is sandwiched between two barrier layers where the sensor detects and sequesters protease, while the barrier captures the released fluorophore. Each layer of the bandage contributes to maintaining moisture via its open semipermeable structure. (b) The first row images depict pCPC, pNCC, and pNA without the top barrier and top layer; the second row images illustrate the top barrier and top layer of the protease sensors with ultraviolet illumination. (c) Shows the HNE reaction path that hydrolyzes the substrate peptide bond scissile to the COOH-terminal fluorophore.[30]

The pNAs have lower detection sensitivity (0.13 U/ml) than the pNC (0.015U/ml), which may be attributable to pore size restriction limiting the HNE enzyme's penetration into the NA structure interior to react with the peptide substrate. On the other hand, the aerogel sensor achieves a higher level of protease sequestration compared to CPC and NCC due to its increased porosity, negative charge, and higher swelling capacity. The NA swelling capacity compensates for its lower surface charge (−36 mV) compared to the NC (−43 mV) by absorbing and increasing the interaction between the wound-like fluid and the NA (Figure 7). The proposed nanocellulosic materials, as well as the CPC, have a 1- to 5-fold increase in sequestering protease than a commercially available protease sequestrant dressing (Figure 7). Therefore, the structures of CPC, NCCs, and the nanocellulose aerogel demonstrate promise for a potential wound dressing interface as a biosensor layer that would also function as protease sequestrant.

Interfacing nanocellulosic biosensors into an in situ paradigm as a dressing motif

The approach of using a sensor with attenuated protease sensitivity interfaced to a protease-modulating dressing is consistent with monitoring occupied elastase binding sites in the protease sequestrant dressing, which is saturated with wound fluid during the time interval of wound treatment.[19] This type of application is also aligned with efforts to develop new-targeted approaches to ensure protease-modulating dressings are functioning optimally. Although there have been a few clinical reports of success treating chronic wounds with protease-modulating dressings,[68] or topical antibiotics that inhibit proteases,[69] reports of using in situ protease sensors to clinically monitor the efficacy of dressing treatments are scarce to none. It is worth noting that although the elastase sensitivity level of the pCPC sensor is too low to detect the concentration of HNE in the medium to low range of chronic wound fluid (0.02–0.1 U/ml).[12,44] It is an example of a weakly sensitive sensor that might serve to signal protease saturation capacity in a protease-modulating dressing. The use of this type of approach is viewed as especially beneficial when used with other combined therapies such as recombinant growth factors or targeted combining therapies where high protease levels in wound fluid inhibit therapy efficacy.[19,54,70]

Interfacing the biosensors into a dressing motif entails a multilayered bandage design as previously reported.[58] Figure 9(a) shows the prototype dressing with multiple layers including a contact, barrier, nanocellulosic biosensor, and top layer. The interchangeable biosensor design is applicable for the wNCC and NA, or even for CPC, see Figure 9(b), which depicts the interfacing of the biosensors in a multilayered wound dressing.

The layers of the dressing/sensor motif have different roles. For example, the wound contact provides exudate absorption, thereby allowing the wound protease-containing exudate to proceed through the barrier layer to the biosensor layer. The insertion of nanocellulosic materials (Figure 9) between the two barrier layers allows entrapment and prevents backwashing of the sensor's signal molecule (fluorophore) into the wound bed. The biosensor layer contains the fluorescent elastase peptide substrate that activates at the threshold levels of the protease titer and sequesters positively charged proteases.

Figure 9(b) shows an image of the pCPC, pNCC, and pNA interfaced into a multilayered intelligent protease sequestrant dressing. The fluorescent detection method is achieved by (i) activation via a handheld long wave ultraviolet light or (ii) removal of the bandage from the wound bed and analysis of the dressing with a long wave ultraviolet light, see Figure 8(b) second row. Figure 9(c) depicts the mode of action pathway of HNE reacting with the peptide substrates anchored onto the cellulosic or nanocellulosic transducer. The HNE substrate binds at the C-terminus of the carbonyl amino bond of the peptide substrate, and cleaves the 7-amino-4-methylcoumarin fluorophore. Illumination of the dressing indicates that the presence of the HNE protease is within the sensitivity limits of the biosensor. The wound-dressing motif provides a new approach to detect HNE present in the wound and to sequester proteases as a POC regimen for evaluating and treating chronic wounds.

The potential benefit of incorporating biosensors into dressings is twofold considering that the biosensors are interfaced with a surface that also treats the chronic wound. The nanocellulosic materials provide enhanced sequestration compared to a commercially available protease sequestrant dressing, and further suggests that protease modulating dressings now being employed clinically can be improved.

Conclusions

Here we have evaluated cellulosic and nanocellulosic materials as an interface for a multilayered intelligent protease sequestrant wound dressing for chronic wounds. The proposed dressing both detect and sequester proteases in a simulated wound-like fluid solution via the use of CPC (control) and nanocellulosic materials (NCs, NCCs, and NAs). The nanocellulosic materials were selected because of their (i) structural and biophysical similarities to commercially available dressings, i.e., gauze, films, and hydrogels, (ii) their

favorable permeability, moisture retention, charge properties, and/or sensor functions, and (iii) their SSA, peptide loading, detection sensitivity, surface charge for sequestration purposes, and permeability as a function of a biosensor layer.

Despite the limited clinical studies that define diagnostic and treatment parameters for wound protease therapy there has been ample reason to treat chronic wounds with protease modulating dressings as evidenced by their widespread use and commercialization.[70] More precise diagnostic and treatment criteria are required to advance the clinical use of POC protease diagnostic/dressing approaches. However, identifying and lowering elevated proteases in patients with chronic wounds is an acceptable approach to correcting a biochemical defect that hinders successful wound therapy. Thus, this study has presented the option of placing different types of protease sensor materials as dressing interfaces based on cellulose and nanocellulose to detect dressing bound protease. Undoubtedly, there are numerous approaches for utilizing this type of design, and it is envisioned that it would benefit wound treatment options some of which have been outlined in this paper. Furthermore, interfacing the nanocellulosic biosensor with an intelligent dressing paradigm is adaptable to the detection of other biomarkers of clinical interest as well, via substitution of the biomolecule with a targeted POC approach.

Author contributions

K. R. F. designed the experiments, synthesized all peptide modified nanocellulose aerogel derivatives, performed all of the material characterization and bioactivity experiments, analyzed the data, conducted literature searches, designed the graphics, wrote the manuscript. J. V. E. conceived the idea of the project, edited the manuscript, and is the corresponding author of the manuscript. D. H. prepared the unmodified nanocellulose composites. N. P. and F. L. prepared the unmodified nanocellulose aerogels and contributed to editing the manuscript, respectively. D.Y. and H.Q. performed the fibroblast experiment. B. D. C. provided funding and management that contributed reagents/materials, analysis tools, and personnel resources to the project.

Acknowledgements

The U.S. Department of Agriculture financed this project. Mention of trade names, commercial products, or methods in this article is solely for providing specific information and does not imply recommendation or endorsement by the U.S. Department of Agriculture.

Declaration of Conflicting Interests

The author(s) declared no potential conflicts of interest with respect to the research, authorship, and/or publication of this article.

Funding

The author(s) received no financial support for the research, authorship, and/or publication of this article.

References

1. MedMarket Diligence, LLC. Advanced medical technologies: Insights, perspectives and inside data from medtech market analysis. WordPress 2013, www.blog.mediligence.com/2013/06/10/wound-management-an-18-5-billion-worldwide-market-in-2021 (accessed 27 September 2017).
2. Suvarna K and Munira M. Wound healing process and wound care dressings: a detailed review. *J Pharm Res* 2013; 2: 6–12.
3. Skórkowska-Telichowska K, Czemplik M, Kulma A, et al. The local treatment and available dressings designed for chronic wounds. *J Am Acad Dermatol* 2013; 68: e117–e126.
4. Abrigo M, McArthur SL and Kingshott P. Electrospun nanofibers as dressings for chronic wound care: advances, challenges, and future prospects. *Macromol Biosci* 2014; 14: 772–792.
5. McCarty SM and Percival SL. Proteases and delayed wound healing. *Adv Wound Care* 2013; 2: 438–447.
6. Yoshino S, Nakagami G, Ohira T, et al. Hydrocellular foam dressing increases the leptin level in wound fluid. *Wound Repair Regenerat* 2015; 23: 703–710.
7. Cutting KF. Wound exudate: composition and functions. *Br J Commun Nurs* 2003; 8: S4–S9.
8. Grimstad Ø, Sandanger Ø, Ryan L, et al. Cellular sources and inducers of cytokines present in acute wound fluid. *Wound Repair Regenerat* 2011; 19: 337–347.
9. International consensus. The role of proteases in wound diagnostics. An expert working group review. *Wounds Int* 2011; 1: 1–13. http://www.woundsinternational.com/media/issues/419/files/content_9869.pdf.
10. Yager DR, Chen SM, Ward SI, et al. Ability of chronic wound fluids to degrade peptide growth factors is associated with increased levels of elastase activity and diminished levels of proteinase inhibitors. *Wound Repair Regenerat* 1997; 5: 23–32.
11. Serena TE. Development of a novel technique to collect proteases from chronic wounds. *Adv Wound Care* 2014; 3: 729–732.
12. Serena TE, Cullen BM, Bayliff SW, et al. Defining a new diagnostic assessment parameter for wound care: elevated protease activity, an indicator of nonhealing, for targeted protease-modulating treatment. *Wound Repair Regenerat* 2016; 24: 589–595.
13. Vandenbroucke RE and Libert C. Is there new hope for therapeutic matrix metalloproteinase inhibition? *Nat Rev Drug Discov* 2014; 13: 904–927.
14. Synder RJ, Driver V, Fife CE, et al. Using a diagnostic tool to identify elevated protease activity levels in chronic and stalled wounds: a consensus panel discussion. *Ostomy Wound Manag* 2011; 57/12: 36–46.
15. Moore K, Huddleston E, Stacey MC, et al. Venous leg ulcers—the search for a prognostic indicator. *Int Wound J* 2007; 4: 163–172.

16. Mohanty SP and Kougianos E. Biosensors: a tutorial review. *Potentials IEEE* 2006; 25: 35–40.
17. Gouvea CMCP. Biosensors for health applications. In: Serra PA (ed.) *Biosensors for health, environment and biosecurity*. Rijeka, Croatia: InTech, 2011, pp.71–86.
18. Hall EAH. *Biosensors*. Cambridge, UK: Open University Press, 1990.
19. Edwards JV. Future structure and properties of mechanism-based wound dressing. In: Edwards JV, Buschle-Diller G, Goheen SC (eds) *Modified fibers with medical and specialty applications*. Dordrecht: The Netherlands: Springer, 2006, pp.11–33.
20. Dargaville TR, Farrugia BL, Broadbent JA, et al. Sensors and imaging for wound healing: a review. *Biosens Bioelectr* 2013; 41: 30–42.
21. Kennedy JF and Bunko K. The use of 'smart' textiles for wound care A2. In: Rajendran S (ed.) *Advanced textiles for wound care*. Cambridge, UK: Woodhead Publishing, 2009, pp.254–274.
22. Palamand S, Brenden R and Reed A. Intelligent wound dressings and their physical characteristics. *Wounds: Compend Clin Res Pract* 1992; 3: 149–156.
23. Korkmaz B, Horwitz MS, Jenne DE, et al. Neutrophil elastase, proteinase 3, and cathepsin G as therapeutic targets in human diseases. *Pharmacol Rev* 2010; 62: 726–759.
24. Edsberg LE, Wyffels JT, Brogan MS, et al. Analysis of the proteomic profile of chronic pressure ulcers. *Wound Repair Regenerat* 2012; 20: 378–401.
25. Dargaville TR, Farrugia BL, Broadbent JA, et al. Sensors and imaging for wound healing: a review. *Biosens Bioelectron* 2013; 41: 30–42.
26. World Union of Healing Societies. Principlies of best practice: diagnostics and wounds. *A consensus document* 2008; Vol 1, pp.1–10. Medical Education Partnership (MEP) Ltd.
27. Derikvand F, Yin DT, Barrett R, et al. Cellulose-based biosensors for esterase detection. *Analyt Chem* 2016; 88: 2989–2993.
28. Patrick AG and Ulijn RV. Hydrogels for the detection and mangement of protease levels. *Macromol Biosci* 2010; 10: 1184–1193.
29. Schyrr B, Boder-Pasche S, Ischer R, et al. Fiber-optic protease sensor based on the degradation of thin gelatin films. *Sens Bio-Sens Res* 2015; 3: 65–73.
30. Edwards JV, Fontenot KR, Prevost N, et al. Synthesis and assessment of peptide-nanocellulosic biosensors. In: Mondal IH (ed.) *Nanocellulose, cellulose nanofibers and cellulose nanocomposites: synthesis and applications*. New York: Nova Science, 2016, pp.475–494.
31. Ciolacu D, Ciolacu F and Popa VI. Amorphous cellulose—structure and characterizatoin. *Cell Chem Technol* 2011; 45: 13–21.
32. Edwards JV, Castro NJ, Condon B, et al. Chromatographic and traditional albumin isotherms on cellulose: a model for wound protein adsorption on modified cotton. *J Biomater Appl* 2012; 26: 939–961.
33. Orelma H, Filpponen I, Johansson L-S, et al. Modification of cellulose films by adsorption of CMC and chitosan for controlled attachment of biomolecules. *Biomacromolecules* 2011; 12: 4311–4318.
34. Dabiri G, Damstetter E and Phillips T. Choosing a wound dressing based on common wound characteristics. *Adv Wound Care* 2016; 5: 32–41.
35. Dodson B. Wood pulp extract stronger than carbon fiber or kevlar, 2012. US Forest Service, http://newatlas.com/cellulose-nanocrystals-stronger-carbon-fiber-kevlar/23959/ (accessed 27 September 2017).
36. Sehaqui H, Zhou Q, Ikkala O, et al. Strong and tough cellulose nanopaper with high specific surface area and porosity. *Biomacromolecules* 2011; 12: 3638–3644.
37. Lahiji RR, Reifenberger R, Moon RJ, et al. Characterization of cellulose nanocrystals by SPM. In: *NSTI nanotechnology conference and trade show: life sciences, medicine & bio materials*. Boston, MA: Nano Science and Technology Institute, 2008, pp. 704–707.
38. Peng Y, Gardner DJ, Han Y, et al. Drying cellulose nanocrystal suspensions. In: Postek MT, Moon RJ, Rudie AW, et al. (eds) *Production and applications of cellulose nanomaterials*. Georgia: TAPPI Press, 2013, pp.31–33.
39. Reiner RS and Rudie AW. Process scale-up of cellulose nanocrystal production to 25 kg per batch at the forest products laboratory. In: Postek MT, Moon RJ, Rudie AW, et al. (eds) *Production and applications of cellulose nanomaterials*. Peachtree Corners, GA: TAPPI Press, 2013, pp.21–24.
40. Edwards JV, Fontenot KR, Haldane D, et al. Human neutrophil elastase peptide sensors conjugated to cellulosic and nanocellulosic materials: part I, synthesis and characterization of fluorescent analogs. *Cellulose* 2016; 23/2: 1283–1295.
41. Hoepfner S, Ratke L and Milow B. Synthesis and characterisation of nanofibrillar cellulose aerogels. *Cellulose* 2008; 15: 121–129.
42. Pircher N, Carbajal L, Schimper C, et al. Impact of selected solvent systems on the pore and solid structure of cellulose aerogels. *Cellulose* 2016; 23: 1949–1966.
43. Sescousse R, Gavillon R and Budtova T. Aerocellulose from cellulose–ionic liquid solutions: preparation, properties and comparison with cellulose–NaOH and cellulose–NMMO routes. *Carbohydr Polym* 2011; 83: 1766–1774.
44. Edwards JV, Fontenot KR, Prevost NT, et al. Preparation, characterization and activity of a peptide-cellulosic aerogel protease sensor from cotton. *Sensors* 2016; 16: 1789–1808.
45. Edwards JV, Prevost NT, French AD, et al. Kinetic and structural analysis of fluorescent peptides on cotton cellulose nanocrystals as elastase sensors. *Carbohydr Polym* 2015; 116: 278–285.
46. Touzinsky GF and Gordon SM. Degree of subsitution of cellulose derivatives containing n different substituent groups. *Carbohydr Res* 1979; 69: 327–329.
47. Brunauer S, Emmett PH and Teller E. Adsorption of gases in multimolecular layers. *J Am Chem Soc* 1938; 60: 309–319.
48. Sehaqui H, Zimmermann T and Tingaut P. Hydrophobic cellulose nanopaper through a mild esterification procedure. *Cellulose* 2014; 21: 367–382.
49. Fontenot KR, Edwards JV, Haldane D, et al. Human neutrophil elastase detection with fluorescent peptide

sensors conjugated to cellulosic and nanocellulosic materials: part II, structure/function analysis. *Cellulose* 2016; 23: 1297–1309.
50. Edwards V, Condon B, Sawhney P, et al. Electrokinetic analysis of hydroentangled greige cotton–synthetic fiber blends for absorbent technologies. *Text Res J* 2013; 83/18: 1949–1949.
51. Lavoine N, Desloges I, Dufresne A, et al. Microfibrillated cellulose—its barrier properties and applications in cellulosic materials: a review. *Carbohydr Polym* 2012; 90: 735–764.
52. Trengove NJ, Langton SR and Stacey MC. Biochemical analysis of wound fluid from nonhealing and healing chronic leg ulcers. *Wound Repair Regenerat* 1996; 4: 234–239.
53. Spence K, Habibi Y and Dufresne A. Nanocellulose-based composites. In: Kalia S, Kaith BS, Kaur I (eds) *Cellulose fibers: bio- and nano-polymer composites: green chemistry and technology*. Heidelberg: Springer, 2011, p.179.
54. Edwards JV, Yager DR, Cohen IK, et al. Modified cotton gauze dressings that selectively absorb neutrophil elastase activity in solution. *Wound Repair Regenerat* 2001; 9: 50–58.
55. Vachon DJ and Yager DR. Novel sulfonated hydrogel composite with the ability to inhibit proteases and bacterial growth. *J Biomed Mater Res Part A* 2006; 76A: 35–43.
56. Edwards JV and Prevost N. Thrombin production and human neutrophil elastase sequestration by modified cellulosic dressings and their electrokinetic analysis. *J Function Biomater* 2011; 2: 391–413.
57. Schoukens G. Bioactive dressings to promote wound healing. In: Rajendran R (ed.) *Advanced textiles for wound care*. Oxford: Woodhead Publishing, 2009, pp.114–152.
58. Edwards JV, Fontenot KR, Prevost NT, et al. Protease biosensors based on peptide-nanocellulose conjugates: from molecular design to dressing interface. *Int J Med Nano Res* 2016; 3/2: 1–11.
59. Winter GD. Formation of the scab and the rate of epithelization of superficial wounds in the skin of the young domestic pig. *Nature* 1962; 193: 293–294.
60. Krasner DL, Sibblald RG and Woo KY. Wound dresing product selection: a holistic interprofessional patient-centered approach. In: Krasner DL, Rodeheaver GT, Sibbald RG, et al. (eds) *Chronic wound care: a clinical source book for healthcare professions*, 5th ed. Malvern, PA: HMP Communications, 2012, pp.223–230.
61. Uzun M, Anand SC and Shah T. In vitro characterisation and evaluation of different types of wound dressing materials. *J Biomed Eng Technol* 2013; 1: 1–7.
62. Dale J. Wound dressings. *Prof Nurs* 1997; 12: 12–18.
63. Xu R, Xia H, He W, et al. Controlled water vapor transmission rate promotes wound-healing via wound re-epithelialization and contraction enhancement. *Scient Rep* 2016; 6: 24596.
64. Rolstad BS and Ovington LG. Principles of wound managment current managment concepts. In: Bryant R, Nix D (eds) *Acute and chronic wounds*. St. Louis, MO: Mosby Elsevier, 2007, pp.391–426.
65. Mautner A, Lee K-Y, Tammelin T, et al. Cellulose nanopapers as tight aqueous ultra-filtration membranes. *Reactive Funct Polym* 2015; 86: 209–214.
66. Thomas S. Wounds and wound healing. In: Thomas S (ed.) *Wound management and dressings*. London: Pharmaceutical Press, 1990, pp.1–14.
67. Wu P, Fisher AC, Foo PP, et al. In vitro assessment of water vapour transmission of synthetic wound dressings. *Biomaterials* 1995; 16: 171–175.
68. Lazaro-Martinez JL, Garcia-Morales E, Beneit-Montesinos JV, et al. Tandomized compartive trial of a collagen/oxidized regenerated cellulose dressing in the treatment of neuropathic diabetic food ulcers. *Ciurgia Espanola* 2007; 82: 27–37.
69. Chin GA, Thigpin TG, Perrin KJ, et al. Treatment of chronic ulcers in diabetic patients with a topical metalloproteinase inhibitor, doxycycline. *Wounds* 2003; 15: 315–323.
70. Cowan L, Stechmiller J, Phillips P, et al. Science of wound healing: translation of bench science into advances for chronic wound care. In: Krasner DL, Rodeheaver GT, Sibbald RG, et al. (eds) *Chronic wound care: a clinical source book for healthcare professions*, 5th ed. Malvern, PA: HMP Communications LLT, 2012, pp.25–35.